Fitting Pole-zero Micromechanical Models to Cochlear Response Measurements

Stephen J Elliott [1], Guangjian Ni* [2,3,1] and Luyang Sun [4,1]

1. Institute of Sound and Vibration Research, University of Southampton, Highfield Campus, Southampton SO17 1BJ United Kingdom
2. Lab of Neural Engineering & Rehabilitation, Department of Biomedical Engineering, College of Precision Instruments and Optoelectronics Engineering, Tianjin University, Tianjin 300072 China
3. Tianjin International Joint Research Center for Neural Engineering, Academy of Medical Engineering and Translational Medicine, Tianjin University, Tianjin 300072 China
4. Key Laboratory of Noise and Vibration Research, Institute of Acoustics, Chinese Academy of Sciences, Beijing 100190 China

Running title: pole-zero models of cochlear micromechanics

Abstract

An efficient way of describing the linear micromechanical response of the cochlea is in terms of its poles and zeros. Pole-zero models with local scaling symmetry are derived for both one and two degree-of-freedom micromechanical systems. These elements are then used in a model of the coupled cochlea, which is optimised to minimise the mean square difference between its frequency response and that measured on the basilar membrane inside the mouse cochlea by Lee *et al*. (2015), at different excitation levels. A model with two degree-of-freedom micromechanics generally fits the measurements better than a model with single degree-of-freedom micromechanics, particularly at low excitations where the cochlea is active, except post-mortem conditions, when the cochlea is passive. The model with the best overall fit to the data is found to be one with two degree-of-freedom micromechanics and 3D fluid coupling. Although a unique lumped parameter network cannot be inferred from such a pole-zero description, these fitted results help indicate what properties such a network should have.

I. INTRODUCTION

It is useful to develop mathematical models of the mechanics of the cochlea in order to test our understanding of the physical processes involved in hearing. The level of detail in these models varies considerably. Finite element methods allow models with a detailed geometry and have been used, for example, to investigate fluid coupling (Böhnke and Arnold, 1999; Cai and Chadwick, 2003; Ni and Elliott, 2015), to study the micromechanical behaviour of the organ of Corti (Kolston and Ashmore, 1996; Cai *et al.*, 2004; Ni *et al.*, 2016) and to study the detailed dynamics of the stereocilia (Baumgart *et al.*, 2008; Kozlov *et al.*, 2011). As a less detailed level, box models of the whole cochlea have been widely used and display many of the important features seen in the overall mechanics of the cochlea, particularly tonotopy and forward and backward travelling waves (de Boer, 1980; Watts, 2000). Box models typically include analytical models of either one-dimensional, 1D, or three-dimensional, 3D, fluid coupling and a locally reacting model of the micromechanics, derived from a lumped parameter representation of the organ of Corti for example (Steele and Taber, 1979; de Boer, 1996). In the passive cochlea, the local micromechanics are generally modelled as a single degree-of-freedom mechanical system, consisting of a local mass, stiffness and damping, whose values vary with position along the cochlea (de Boer, 1996; Hubbard and Mountain, 1996). Several two degree-of-freedom micromechanical models have also been used to represent the active cochlea with either an explicit or implicit representation of the feedback process that provides the cochlear amplifier (Neely and Kim, 1986; Geisler, 1993; Liu and Neely, 2009). Although the response of the cochlea is known to change with excitation level, it behaves almost linearly when driven at given level of excitation (de Boer, 1997) and so quasi-linear models , in which a linear model is assumed with parameters that change with the level of excitation (Kanis and de Boer, 1993; Liu, 2014), have been widely used to quantify the cochlear response. Such quasi-linear models are a particularly good representation of the underlying nonlinear system if the nonlinearity is associated with the damping (Elliott *et al.*, 2015).

Yet more abstract models do not concern themselves with the detailed mechanisms that give rise to the local dynamic behaviour, but describe the micromechanical response in terms of its poles and zeros (Zweig, 1991, 2015; Mandal *et al*., 2009). Zweig (1991) originally assumed an active micromechanical model with negative damping stabilised by a time-delayed stiffness, and considered the poles of the organ of Corti admittance. He showed that the dominant response was from a pair of closely-spaced poles close to the frequency axis, as also emphasised in Zweig (2015). Mandal *et al*. (2009) approximated the form of the admittance

proposed by Zweig (1991) by assuming two coincident pairs of poles. A pole-zero model will generally have fewer parameters than an equivalent mechanical model, as illustrated in the example in Section II, so that it provides an efficient representation of the micromechanical behaviour. It is thus of interest to investigate the potential for fitting a cochlear model with a pole-zero representation of the micromechanics to measurements of coupled basilar membrane, BM, response. Even if this does not directly lead to a mechanical model of the cochlea, at least it helps to define the types of behaviour that this micromechanical model must display.

In this paper pole-zero micromechanical models are derived that obey scaling symmetry (Zweig, 1991). These are then used in a coupled cochlear model, with either one or two degree-of-freedom and with either 1D or 3D fluid coupling, and fitted to the basilar membrane responses measured at different excitation levels in intact mouse cochleae by Lee *et al.* (2015). The technique could be viewed as a variation of the "inverse" methods that have previously been used to infer, from measured cochlear responses, either the frequency responses of the BM admittance (Diependaal *et al.*, 1986; Zweig, 1991; de Boer, 1995) or the local variation of the complex wavenumber (Shera, 2007). A preliminary version of this work, applied to measurements from the chinchilla, was presented by Sun *et al.* (2015), and a subset of the results reported here was described by Elliott *et al*. (2017).

Section II describes the derivation of pole-zero descriptions of single and two degree-of-freedom micromechanical models, with the well-known model of Neely and Kim (1986) considered as a special case of the general formulation. The pole-zero fitting procedure for measured data is described in Section III and the results assuming 1D fluid coupling are presented in Section IV. The results of assuming 3D fluid coupling are then presented in Section V. Both single and two degree-of-freedom micromechanical models are considered and the overall quality of the fit is quantified using the normalised mean square error, as discussed in Section VI.

II. POLE-ZERO DESCRIPTIONS OF ONE AND TWO DEGREE-OF-FREEDOM MODELS OF THE MICROMECHANICS

The purpose of this section is to illustrate the connection between a description of the micromechanics in terms of the dynamics of a lumped parameter system, and a description in terms of its underlying poles and zeros.

A. Passive single degree-of-freedom micromechanical model

We begin with the micromechanical model that is widely used to describe the basilar membrane dynamics in the passive cochlea, which has a single degree-of-freedom. The ratio of the BM velocity at position x along the cochlea to the pressure difference at this point can be written as the local BM admittance[1],

$$Y_{\mathrm{BM}}(x,s) = \frac{s}{k(x)+sc(x)+s^2m(x)}, \quad (1)$$

where $k(x)$, $c(x)$ and $m(x)$ are the local stiffness, damping and mass per unit area of the BM. The Laplace variable s is complex and is equal to $i\omega$ in the case of sinusoidal excitation at an angular frequency of ω, but the Laplace transform also allows the response to be calculated for arbitrary excitations (see, for example, Kuo, 1966).

This admittance can also be written in terms of the natural frequency, $\omega_0(x)$, and the Q factor, $Q_0(x)$, of the single degree-of-freedom system,

$$Y_{\mathrm{BM}}(x,s) = \frac{s}{m(x)\left[s^2+s\omega_0(x)/Q_0(x)+\omega_0^2(x)\right]}, \quad (2)$$

where $\omega_0(x)$ is equal to $\sqrt{k(x)/m(x)}$ and $Q_0(x)$ is equal to $\sqrt{k(x)m(x)}/c(x)$. We now assume that the BM mass is independent of the local position, so $m(x)$ is equal to m_0, and that the micromechanics satisfy local scaling symmetry (Zweig, 1991; Shera, 2007), so that the Q factor is also constant, with $Q_0(x)$ is equal to Q_0, and the natural frequency of the BM scales with the characteristic frequency, CF, along the cochlea. If $\omega_{\mathrm{n}}(x)$ is equal to 2πCF at the position x, we can write the BM natural frequency as,

$$\omega_0(x) = \Omega_0\omega_n(x), \quad (3)$$

where Ω_0 is the normalised natural frequency, which is assumed to be independent of x.

The single degree-of-freedom BM admittance which satisfies scaling symmetry can thus be written as

$$Y_{\mathrm{BM}}(x,s) = \frac{s}{m_0\left[s^2+s\Omega_0\omega_{\mathrm{n}}(x)/Q_0+\Omega_0^2\omega_{\mathrm{n}}^2(x)\right]}, \quad (4)$$

[1] Strictly speaking this is the admittance of the whole cochlear partition, not just the BM, but since it is assumed here that it is the BM motion that couples into the fluid in the scalae and this response is fitted to the response of the BM below, it will be termed the BM admittance here to avoid confusion.

The zeros of $Y_{BM}(x, s)$ are defined as the values of the complex variable s that drive $Y_{BM}(x, s)$ to zero, and are given by the roots of the numerator of equation (4). In this single degree-of-freedom case, $Y_{BM}(x, s)$ has a single zero at s=0. The poles of $Y_{BM}(x, s)$ are the values of s that drive it to infinite and are given by the roots of the denominator of equation (4), which gives a pair of poles at

$$s = \Omega_0 \omega_n(x) \left[-\frac{1}{2Q_0} \pm i \sqrt{1 - \frac{1}{4Q_0^2}} \right], \tag{5}$$

which forms a complex conjugate pair if Q is greater than 1/2.

B. A general active two degree-of-freedom model

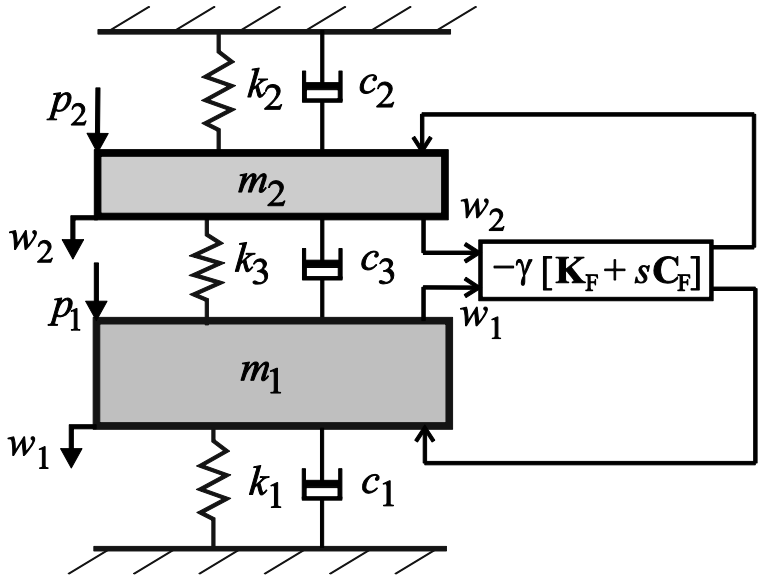

Figure 1 Lumped parameter representation of an active two degree-of-freedom model of the local cochlear micromechanics with general feedback matrix $-\gamma[\mathbf{K}_F+s\mathbf{C}_F]$.

A two degree-of-freedom micromechanical model has two masses, as illustrated in Figure 1. The two masses are assumed to be passively coupled by stiffnesses k_1, k_2 and k_3, and dampers c_1, c_2 and c_3, but also coupled by a matrix of feedback gains representing the active contribution to the response. The explicit dependence of the mass, stiffness and damping on the position within the cochlea, x, is dropped here for notational convenience. Ignoring the feedback terms for the time being, the relationship between the displacements of the two masses, w_1 and w_2, and the total pressures acting on them, p_{T1} and p_{T2}, is given for the passive system by (Warburton, 1976)

$$\begin{bmatrix} p_{T1} \\ p_{T2} \end{bmatrix} = \left[\begin{bmatrix} k_1 + k_3 & -k_3 \\ -k_3 & k_2 + k_3 \end{bmatrix} + s \begin{bmatrix} c_1 + c_3 & -c_3 \\ -c_3 & c_2 + c_3 \end{bmatrix} + s^2 \begin{bmatrix} m_1 & 0 \\ 0 & m_2 \end{bmatrix} \right] \begin{bmatrix} w_1 \\ w_2 \end{bmatrix}. \tag{6}$$

Including the feedback terms, the total pressures acting on the two masses can be written as

$$\begin{bmatrix} p_{\mathrm{T}1} \\ p_{\mathrm{T}2} \end{bmatrix} = \begin{bmatrix} p_1 \\ p_2 \end{bmatrix} - \gamma \left[\begin{bmatrix} k_{11}^{\mathrm{F}} & k_{12}^{\mathrm{F}} \\ k_{21}^{\mathrm{F}} & k_{22}^{\mathrm{F}} \end{bmatrix} + s \begin{bmatrix} c_{11}^{\mathrm{F}} & c_{12}^{\mathrm{F}} \\ c_{21}^{\mathrm{F}} & c_{22}^{\mathrm{F}} \end{bmatrix} \right] \begin{bmatrix} w_1 \\ w_2 \end{bmatrix}, \tag{7}$$

where p_1 and p_2 are the external pressures acting on m_1 and m_2, and k_{11}^{F}, k_{12}^{F}, k_{21}^{F} and k_{22}^{F} represent displacement feedback gains and c_{11}^{F}, c_{12}^{F}, c_{21}^{F} and c_{22}^{F} represent velocity feedback gains which, in matrix notation are denoted as $-\gamma[\mathbf{K}_{\mathrm{F}}+s\mathbf{C}_{\mathrm{F}}]$ in Figure 1. For notational simplicity it is assumed that all of these gains are proportional to a single non-dimensional active gain parameter, γ, which will be a function of excitation level in a quasi-linear model. In general, however, the identification process used below does not require this assumption, since all the elements of $\mathbf{K}_{\mathrm{F}}$ and $\mathbf{C}_{\mathrm{F}}$ could, in principle, vary independently with excitation level. Substituting equation (7) into equation (6), the overall dynamics of the active two degree-of-freedom model can be written as

$$\begin{bmatrix} p_1 \\ p_2 \end{bmatrix} = \left[\begin{bmatrix} k_{11} & k_{12} \\ k_{21} & k_{22} \end{bmatrix} + s \begin{bmatrix} c_{11} & c_{12} \\ c_{21} & c_{22} \end{bmatrix} + s^2 \begin{bmatrix} m_1 & 0 \\ 0 & m_2 \end{bmatrix} \right] \begin{bmatrix} w_1 \\ w_2 \end{bmatrix}, \tag{8}$$

where

$$\begin{aligned} k_{11} &= \gamma k_{11}^{\mathrm{F}} + k_1 + k_3, \quad k_{12} = \gamma k_{12}^{\mathrm{F}} - k_3, \\ k_{21} &= \gamma k_{21}^{\mathrm{F}} - k_3, \qquad k_{22} = \gamma k_{22}^{\mathrm{F}} + k_2 + k_3, \\ c_{11} &= \gamma c_{11}^{\mathrm{F}} + c_1 + c_3, \quad c_{12} = \gamma c_{12}^{\mathrm{F}} - c_3, \\ c_{21} &= \gamma c_{21}^{\mathrm{F}} - c_3, \qquad c_{22} = \gamma c_{22}^{\mathrm{F}} + c_2 + c_3. \end{aligned} \tag{9}$$

It is important to note that whereas the stiffness and damping matrices in equation (6) are symmetric, as they must be for any passive system (Warburton 1976), the feedback terms k_{12}^{F} and c_{12}^{F} are not necessarily equal to k_{21}^{F} and c_{21}^{F}. So that the stiffness and damping matrices for the active system, in equation (8), are not necessarily symmetric, and the system is not necessarily reciprocal.

If m_1 is assumed to represent the mass of the BM, then the external pressure acting on m_1 is due to the pressure difference between the two fluid chambers. It is assumed that since the upper part of the organ of Corti is entirely surrounded by the endolymph, the pressure in this chamber acts on both sides of m_2 and so the net external pressure, p_2, due to this fluid pressure

is zero. In models that assume 1D fluid coupling, then m_1 will also include the mass due to the fluid loading on the BM (Neely, 1985, Elliott *et al*. 2011). If w_2 is interpreted as the motion of the reticular laminar, then the fluid loading would contribute to m_2 and also add off-diagonal terms to the mass matrix above (Elliott and Ni, 2014). It is also possible to generalise the definition of the feedback term in equation (7) to include a mass matrix, which might not be symmetric, due to acceleration feedback. The identification process used below does not require the assumption that the mass matrix is diagonal or symmetric, so this complication is again ignored. So, assuming that p_2 is equal to 0, equation (8) can be solved to give an explicit equation for the ratio of the velocity of m_1, equal to sw_1, to the fluid pressure acting on it, p_1, which is equal to the BM admittance in this case and is given by

$$\frac{sw_1}{p_1} = Y_{\mathrm{BM}}(s) = \frac{s\left(s^2+sc_{22}/m_2+k_{22}/m_2\right)}{m_1[(s^2+sc_{11}/m_1+k_{11}/m_1)(s^2+sc_{22}/m_2+k_{22}/m_2)-(k_{12}+sc_{12})(k_{21}+sc_{21})/m_1m_2]}. \quad (10)$$

where the stiffness and damping coefficients, as given in equation (9), depend on γ and so are level-dependent in a quasi-linear model.

This general form of the two degree-of-freedom admittance has four poles and three zeros. which are given, respectively, by the roots of the fourth-order denominator and the third-order numerator of equation (10). Again assuming scaling symmetry and reintroducing the dependence on x, the admittance of this general two degree-of-freedom active model can be written as

$$Y_{\mathrm{BM}}(x,s) = \frac{s[s^2+\Omega_{\mathrm{Z}}\omega_{\mathrm{n}}(x)s/Q_{\mathrm{Z}}+\Omega_{\mathrm{Z}}^2\omega_{\mathrm{n}}^2(x)]}{m_1[s^2+\Omega_{\mathrm{A}}\omega_{\mathrm{n}}(x)s/Q_{\mathrm{A}}+\Omega_{\mathrm{A}}^2\omega_{\mathrm{n}}^2(x)][s^2+\Omega_{\mathrm{B}}\omega_{\mathrm{n}}(x)s/Q_{\mathrm{B}}+\Omega_{\mathrm{B}}^2\omega_{\mathrm{n}}^2(x)]}, \quad (11)$$

where Ω_{Z} and Q_{Z} are the normalised natural frequency and Q factors of the pair of zeros for the admittance, which also has another zero at s equal to 0, and Ω_{A} and Ω_{B}, and Q_{A}, and Q_{B} are the normalised natural frequencies and Q values of the two pairs of poles.

It is important to note that although the original micromechanical model, in equation (10), has 10 parameters, corresponding to 2 masses, 4 overall stiffnesses and 4 overall dampers, the pole-zero representation of this model, in equation (11), has only 7 parameters, corresponding to an overall mass and the normalised natural frequencies and normalised damping values of two pairs of poles and one pair of zeros. Although the parameters of the poles and zeros in equation (11) can be uniquely calculated from the physical variables in equation (10), a unique set of these physical variables could not be computed if only the complex values of the poles and zeros were known. Of more consequence here is that the pole-zero representation of the BM

admittance requires the smallest possible number of parameters to specify its response, i.e. the response is canonical (Kuo, 1966). Such a pole-zero model can thus be uniquely fitted to measured sets of data with the minimum number of free variables. This fitting procedure is described in Section III.

C. Example of the Neely and Kim active micromechanical model

We now consider a special case of the general two degree-of-freedom model in Section II B, as described by Neely and Kim (1986). In the Neely and Kim model, the active pressure only acts on m_1, so that k_{21}^{F}, k_{22}^{F}, c_{21}^{F} and c_{22}^{F} are zero in equation (7). The active pressure acting on m_1 in the Neely and Kim model is equal to $-\gamma(k_4+sc_4)(w_2-w_1)$, so that in the general model we also have $k_{12}^{\mathrm{F}} = -k_{11}^{\mathrm{F}} = k_4$ and $c_{12}^{\mathrm{F}} = -c_{11}^{\mathrm{F}} = c_4$. By using these values of the feedback terms in the definitions of the stiffness and damping in equation (8), and setting the scaling factor of g/b in Neely and Kim to unity for notational convenience, the general BM admittance in equation (10) can, in this particular case, be written as

$$Y_{\mathrm{BM}}(x,s) = \frac{[Z_2(x,s)+Z_3(x,s)]}{Z_1(x,s)[Z_2(x,s)+Z_3(x,s)]+Z_2(x,s)[Z_3(x,s)-\gamma Z_4(x,s)]}, \tag{12}$$

where

$$\begin{aligned} Z_1(x,s) &= k_1(x)/s + c_1(x) + sm_1(x), \\ Z_2(x,s) &= k_2(x)/s + c_2(x) + sm_2(x), \\ Z_3(x,s) &= k_3(x)/s + c_3(x), \\ Z_4(x,s) &= k_4(x)/s + c_4(x). \end{aligned} \tag{13}$$

Using the parameters suggested by Neely and Kim at a position that is 13 mm along the cochlea, for which the characteristic frequency is about 3.4 kHz, the poles and zeros of this micromechanical model can be calculated from the roots of the numerator and denominator of equation (12), for different values of the feedback gain, γ. Figure 2 shows the real and imaginary parts of s/ω_{n} that corresponds to complex position of the poles, ×, and zeros, o, for γ equal to 0, i.e. fully passive, 0.5, 0.85 and 1.0, i.e. fully active.

It is interesting to note that the positions of the zeros in the Neely and Kim model do not change with feedback gain, since the numerator of equation (12) is independent of γ. In terms of the general model in Section II B, this is because both k_{22} and c_{22} in equation (8), which appear in the numerator of equation (10) and are defined in equation (9), are independent of γ, since both

k_{22}^{F} and c_{22}^{F} are zero in the Neely and Kim model. Physically, it is the dynamic behaviour of the mechanical system above m_1 in Figure 1 that determines the positions of the zeros of Y_{BM} (Warburton 1976), and since there is no active force acting on m_2 in the Neely and Kim model, its dynamics are independent of the feedback gain. We will see that when the general two degree-of-freedom micromechanical model is fitted to the measured data, the positions of the zeros, as well as the poles, do change with excitation level, indicating that in this case the feedback pressures act on both m_1 and m_2.

It can also be seen from Figure 2 that when γ is equal to 0, and the system is passive, one pair of poles is almost coincident with the complex pair of zeros. The effect of these pairs of poles and zeros are thus almost cancelled out in the response, which appears as if it was a single degree-of-freedom system. Physically, this is because k_3 is large compared to k_1 and k_2 in the Neely and Kim model, so that without any feedback the two masses, m_1 and m_2, almost move together as a single element. As the feedback gain increases, this pair of poles progressively move away from the positions of the pair of zeros, and since these poles and zeros are closer to the imaginary axis than the other pair of poles, they have a greater effect on the micromechanics (Kuo, 1966), and hence on the overall coupled response of the cochlea. The excitation due to the feedback then forces m_1 to behave differently from m_2, generating the second mode of this two degree-of-freedom system.

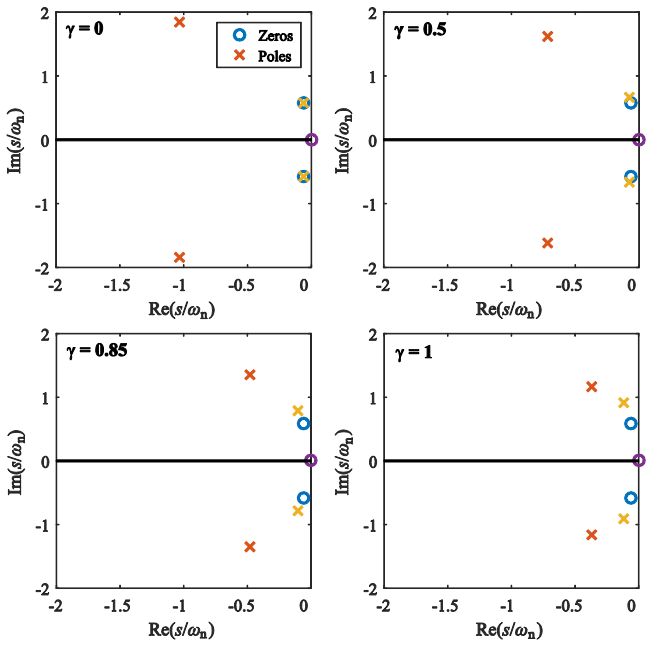

Figure 2 (colour online) The normalised positions of the four poles, ×, and the three zeros, o, in the Neely and Kim micromechanical model, at x=13 mm, for values of feedback gain equal to 0, i.e. fully passive, 0.5, 0.85 and 1.0, i.e. fully active.

III. FITTING POLE-ZERO MICROMECHANICAL MODELS TO MEASURED BM FREQUENCY RESPONSES

Many measurements have been made of the frequency response of the BM motion at given locations along the opened cochlea of laboratory animals. These measurements were originally made using Mössbauer methods (Rhode, 1971; Sellick *et al*., 1982) and later, and most extensively, using laser techniques (Nuttall *et al*., 1991; Mammano and Ashmore, 1993; Nilsen and Russell, 2000; Ren and Nuttall, 2001; Ren, 2002). More recently optical coherence tomography, OCT, has been used to measure the response at various positions in the intact cochlea (Choudhury *et al*., 2006; Wang and Nuttall, 2010; Gao *et al*., 2013; Lee *et al*., 2015, 2016). The results of these OCT measurements of the BM frequency response have a similar form to the earlier laser measurements, but may be more reliable, since in this case the cochlea is still intact and so the action of the cochlear amplifier is not compromised by opening the fluid chambers. The BM response changes with sound pressure level, SPL, due to its quasi-linear behaviour, as described in the Introduction. In order to investigate the complexity of the model needed to match these experimental measurements, it is of interest to fit different orders of micromechanical model to these measurements. The BM frequency response measurements used here were taken from the website[2] associated with the paper by Lee *et al*. (2015), who measured them at 4 closely-spaced locations in intact mouse cochlea at different levels, and also post-mortem, using swept frequency stimulations.

Even if a pole-zero model for the micromechanics is adopted, with a minimum number of free parameters, there are still a number of problems to be overcome in the fitting procedure. The first is that the pole-zero model only describes the isolated micromechanical behaviour at a single position along the cochlea and yet the measured results are from the longitudinally coupled cochlea. The approach adopted here is to assume scaling symmetry, so that the natural frequencies and Q factors of the poles and zeros scale with the characteristic frequency along the cochlea, at least locally around the measurement point. The approach implicitly assumes that the feedback gain is also locally constant around the measurement position. This is not unreasonable for harmonic excitation, since the feedback gain only significantly affects the BM admittance at frequencies close to the characteristic place, and the BM response is always stiffness control at more basal positions and mass controlled at more apical positions. Then, with a given model of the fluid coupling, which may be either 1D or 3D; the coupled response

[2] Oghalai Lab https://oghalailab.stanford.edu/, accessed on 6 July 2016.

of an elemental box model can be calculated (Elliott *et al*., 2011) and compared with the measured results, as shown in Figure 3. Since the response of the cochlea is assumed to be linear, at a given driving SPL, the predicted BM velocity at elemental positions all along the cochlea can be easily calculated at a given driving frequency using simple matrix methods (Neely, 1981; Elliott *et al.*, 2007).

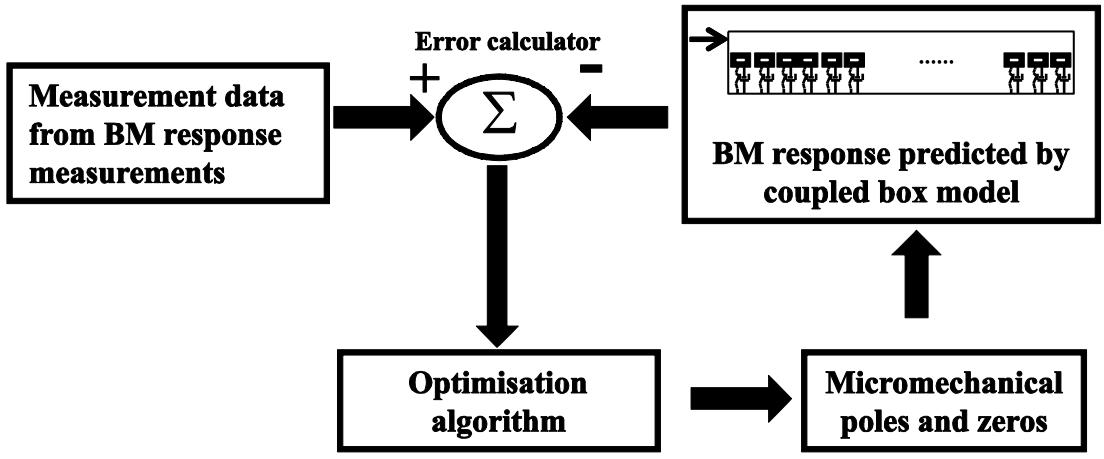

Figure 3 The block diagram used for the optimisation of the micromechanical parameters in a model in order to fit the measured BM response in the coupled cochlea.

The second problem that arises is how to adjust the pole and zero positions in the micromechanical model to best match the calculated coupled response to the measured data, as indicated by the "optimisation algorithm" in Figure 3. A number of numerical optimisation algorithms could be used for this fitting problem, but the algorithm employed here uses the interior-point method, as implemented by the function *fmincon* in Matlab™ (2015b). The cost function that is minimised by this algorithm is the normalised mean square error, NMSE, which in this application is averaged across the number of measurements available, *N*, to give

$$\mathrm{NMSE} = \frac{\sum_{n=1}^{N} |\hat{V}_{\mathrm{BM}}(n) - V_{\mathrm{BM}}(n)|^2}{\sum_{n=1}^{N} |V_{\mathrm{BM}}(n)|^2}, \tag{14}$$

where $V_{\mathrm{BM}}(n)$ is the complex value of the measured BM velocity at the *n*-th measurement frequency and $\hat{V}_{\mathrm{BM}}(n)$ is the complex value of the BM velocity calculated from the numerical model. It should be noted that for this optimisation problem the NMSE is not a convex function of the fitted parameters, so that the optimisation is not guaranteed to have a unique global minimum. In fact the optimisation algorithm requires constraints to be placed on the parameter values to ensure its reliable convergence. One obvious constraint that has to be imposed is that the normalised natural frequency and *Q* factors are positive, beyond this the convergence of the algorithm is found to be most reliable if the parameters are constrained to be between

reasonable upper and lower bounds, which were taken for most of the simulations here to be from 0.1 to 1.5 for the normalised frequency, from 0.1 to 10 for the normalised damping and from 0.01 to 0.3 for the BM mass. The actual tuning was slightly more complicated, however, and the upper and lower bounds used to obtain the lowest NMSE varied somewhat with number of degree-of-freedom, excitation level and measurement position. The optimisation algorithm is found to converge to a reliable solution for different data sets, however, as discussed in Section IV in connection with Figure 5.

Although, in principle, the set of calculated velocities used in the optimisation process could be directly calculated for different frequencies at a given position along the cochlea, to match the measured responses, the numerical model would then have to be run N times, at different frequencies, to give the N values of $\hat{V}_{\mathrm{BM}}(n)$. It is thus far more efficient to use scaling symmetry to convert the measured frequency response at a given cochlear position, to the distribution of BM response along the cochlea when excited at a single frequency (Shera, 2007). This can readily be accomplished using an assumed distribution of characteristic frequency along the cochlea, which is taken here to have the form

$$\mathrm{CF} = f_{\mathrm{B}} e^{-x/l}, \tag{15}$$

where x is the distance away from the base, f_B is the CF at the base of the cochlea, and l is the characteristic length, which for the mouse data used here was assumed to be 105 kHz and 1.5 mm respectively, calculated from the parameters given by Greenwood (1990). Assuming 1D fluid coupling again, the effective height of the scala in the coupled box model was set to 0.5 mm, as given by equation (16) in Elliott *et al*. (2011), when the physical area of the scala is about 0.06 mm^2 (Thorne *et al.*, 1999) and the BM width is about 0.15 mm (Keiler and Richter, 2001).

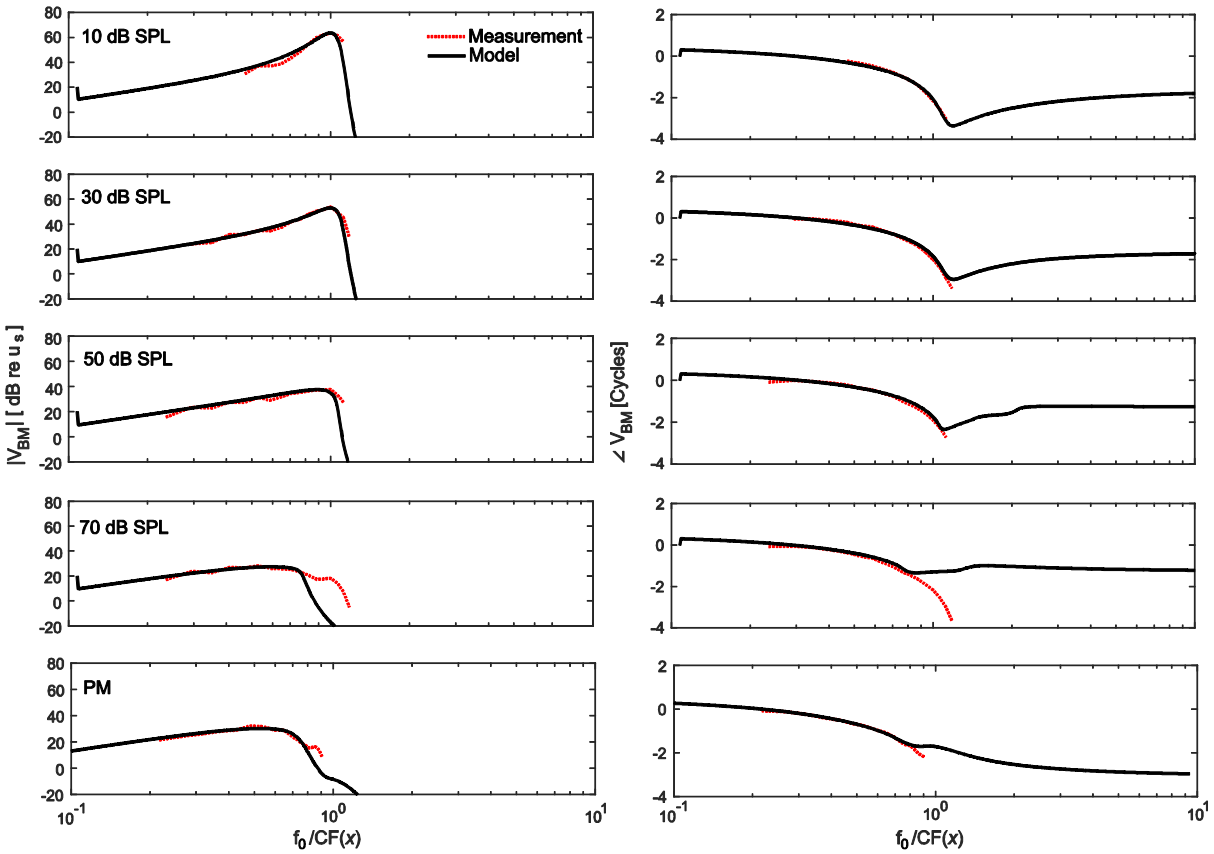

Figure 4 The normalised frequency responses of BM velocity, calculated using scaling symmetry, from the frequency response measured at the position of which CF is 9 kHz and 10, 30, 50, and 70 dB SPL in the mouse by Lee *et al*. (2015) and that fitted from the coupled model having two degree-of-freedom micromechanics and 1D fluid coupling, by minimising the mean square error between the measurements, $V_{\mathrm{BM}}(n)$, and the predictions, $\hat{V}_{\mathrm{BM}}(n)$.

Figure 4, for example, shows a comparison of the magnitude and phase of the measured BM velocity, normalised by the stapes velocity and measured for 4 different SPLs and post-mortem, PM, by Lee *et al*. (2015), together with the coupled response of a box model having two degree-of-freedom micromechanics, with parameters optimised to minimise the mean square error, and 1D fluid coupling. It can be seen that the magnitude is fitted reasonably well, apart from just beyond the peak at high excitation levels. The phase of the coupled models also fit the measured data reasonably well, without the problems, observed by Wang *et al*. (2016), specifically in Figure S2 of their supplementary material. It should be noted that the frequency range of the measured data varies with SPL, due to signal and to noise issues, but that the NMSE is only defined over the frequency range of the measurements. The PM sensitivity functions are reasonably independent of excitation level in the data, as expected, but the results measured at 70 dB SPL were used here since they had the best signal to noise ratio.

IV. POLES AND ZEROS OF THE FITTED MICROMECHANICAL MODEL WITH 1D FLUID COUPLING

A. Results of fitting with a two degree-of-freedom micromechanical model

This fitting procedure, with two degree-of-freedom micromechanics and 1D fluid coupling, has also been applied to the BM response measurements at the three other closely spaced positions along the cochlea reported in the supplementary material of Lee *et al*. (2015), for all excitation levels. The real and imaginary parts of the poles and zeros identified in the models for each of these sets of data are plotted as a function of excitation level in Figure 5. The real and imaginary values of the pole and zero positions, and their variation with excitation level, can be seen to be reasonably consistent across the models fitted to the four sets of data, illustrating the reliability of the optimisation algorithm, apart from the positions of the zeros at low excitation levels and some variation in the imaginary parts of the zeros and one pair of poles at high excitation levels. The first pair of poles, denoted Poles A in Figure 5, was defined to be those with the largest imaginary part, i.e. the pair with the highest normalised frequencies. The BM mass, m_1 in equation (11), identified in these models was about 0.23 kg/m^2, in reasonable agreement with the expected value in a 1D box model, where the BM mass implicitly includes a component due to fluid loading (Neely, 1985; Elliott *et al.*, 2011).

From all of these results, those measured at the position with a CF of about 9 kHz were considered to be most representative of the overall behaviour of the poles and zeros at different excitation levels. The positions of the individual poles and zeros for four different excitation levels in this case are plotted in Figure 6. The identified micromechanical models are all minimum phase since all of their poles and zeros have negative real parts, as expected for the point admittances of a stable system (Kuo, 1966). It is striking that the two pairs of poles are almost coincident in the fully active case, at low SPLs, as predicted theoretically by Zweig (1991, 2015) and as assumed by Mandal *et al*. (2009). At higher excitation levels, the positions of the pairs of zeros approach that the two pairs of poles, which are then no longer almost coincident.

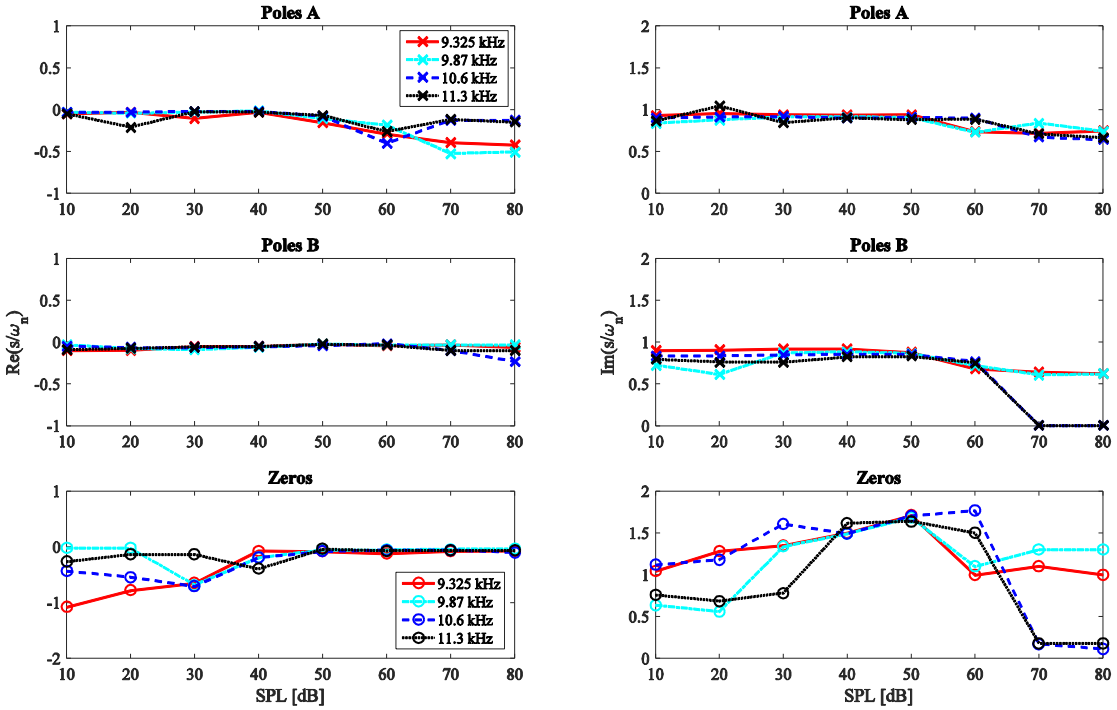

Figure 5 (colour online) The poles and zeros positions of the micromechanical models fitted to the measurements at four different positions, having CFs indicated in the figure, in Lee *et al.* (2015).

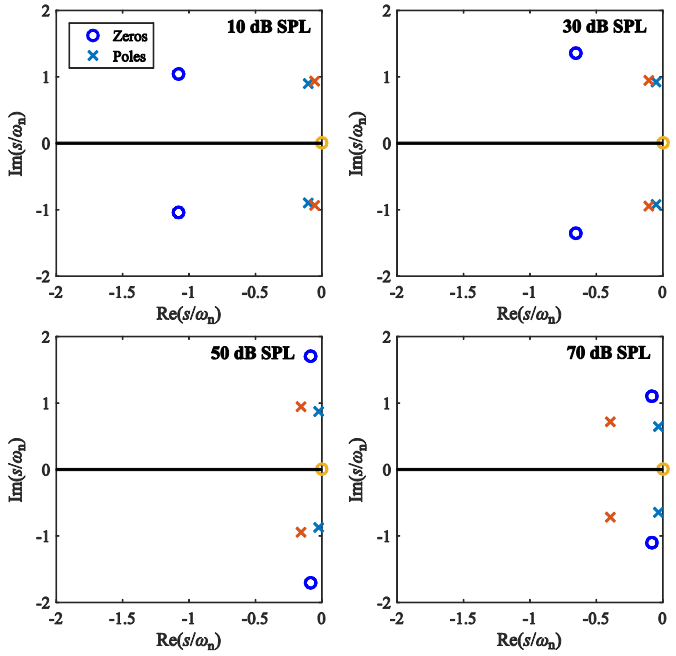

Figure 6 (colour online) Real and imaginary parts of the poles, ×, and zeros, o, calculated from the two degree-of-freedom model with 1D fluid coupling based on measurement data from Lee *et al.* (2015) for the position with a CF of 9 kHz and SPLs of 10, 30, 50 and 70 dB.

It is also noteworthy that the undamped natural frequencies of all the BM admittance poles are nearly equal to CF for levels below 60 dB SPL, i.e. Im(s/ω_n) is nearly unity, so that as the level changes, the pole positions move almost parallel to the real axis in our representation, i.e. at right angles to the frequency axis, as predicted by Shera (2001) as a condition for the times of

the peaks in the corresponding impulse responses being independent of level. With reference to equations (5) and (11), it can be seen that the physical interpretation of this effect is that the normalised natural frequency of the poles does not change significantly with level, but that the Q value does, although the Q value is still large enough for the $1/4Q^2$ term in equation (5) to be negligible. This implies that the velocity feedback terms in equation (7), which affect the damping of the system, have a greater effect than the displacement feedback terms, which would affect the natural frequency. The impulse response of the coupled BM motion can be calculated from the modelled frequency response functions, computed at uniformly spaced frequencies, with the fitted parameters used to plot the responses in Figure 4. These impulse response functions for the fitted data at different excitation levels are shown, in normalised form, in Figure 7. It can be seen that the times of the first few peaks in these responses is reasonably independent of level, except at 70 dB SPL, where the magnitude of the fitted response at CF in Figure 4 does not match the measurements quite so well as it does at lower levels. It is also interesting to note that in contrast to the poles of the BM admittance, which become less damped as the level decreases and the cochlea becomes more active, the zeros of the BM admittance move to the left as the level decreases and so have more damping. The fact that the zeros move at all with level is evidence that feedback forces act on m_2 as well as m_1 in Figure 1, as discussed in Section II C, and a movement almost parallel to the real axis again suggests mainly velocity feedback. From equation (10) it can be seen that the damping of the zeros of the BM admittance are determined by c_{22} , which is itself given, in equation (9), by $\gamma c_{22}^{\mathrm{F}} + c_2 + c_3$. Since this damping term increases with decreasing level this suggests that $\gamma c_{22}^{\mathrm{F}}$ is positive.

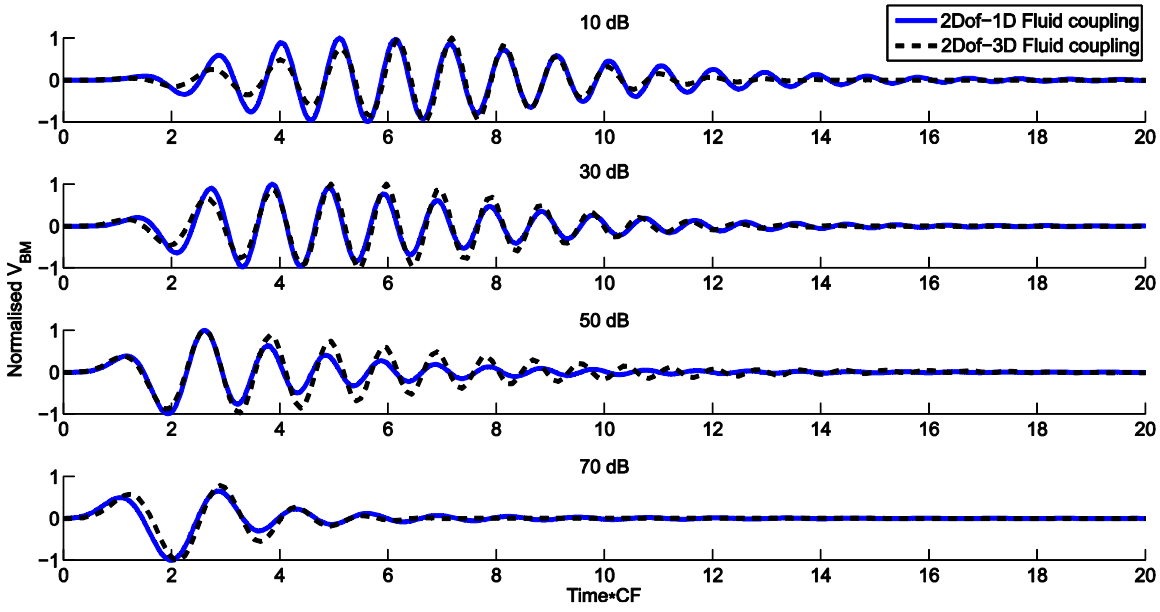

Figure 7 The impulse response of the coupled BM motion, calculated from the inverse Fourier transform of the BM frequency response functions calculated from the fitted responses with 1D fluid coupling in Figure 4 (solid line) and with 3D fluid coupling in Figure 9 (dashed line) at different excitation levels, plotted as a function of normalised time and normalised in amplitude to have a maximum amplitude of unity.

B. Results of fitting with a single degree-of-freedom micromechanical model

The fitting procedure can also be run assuming that the micromechanics of the BM act as a single degree-of-freedom system that obeys scaling symmetry, as in equation (4). The results of fitting the measured data with such a model are shown in Figure 8, and, as expected, the model now reproduces the magnitude of the BM motion better at high SPLs where it is more passive, than it does at low SPLs, which leads to higher values of mean square error, as discussed in Section VI.

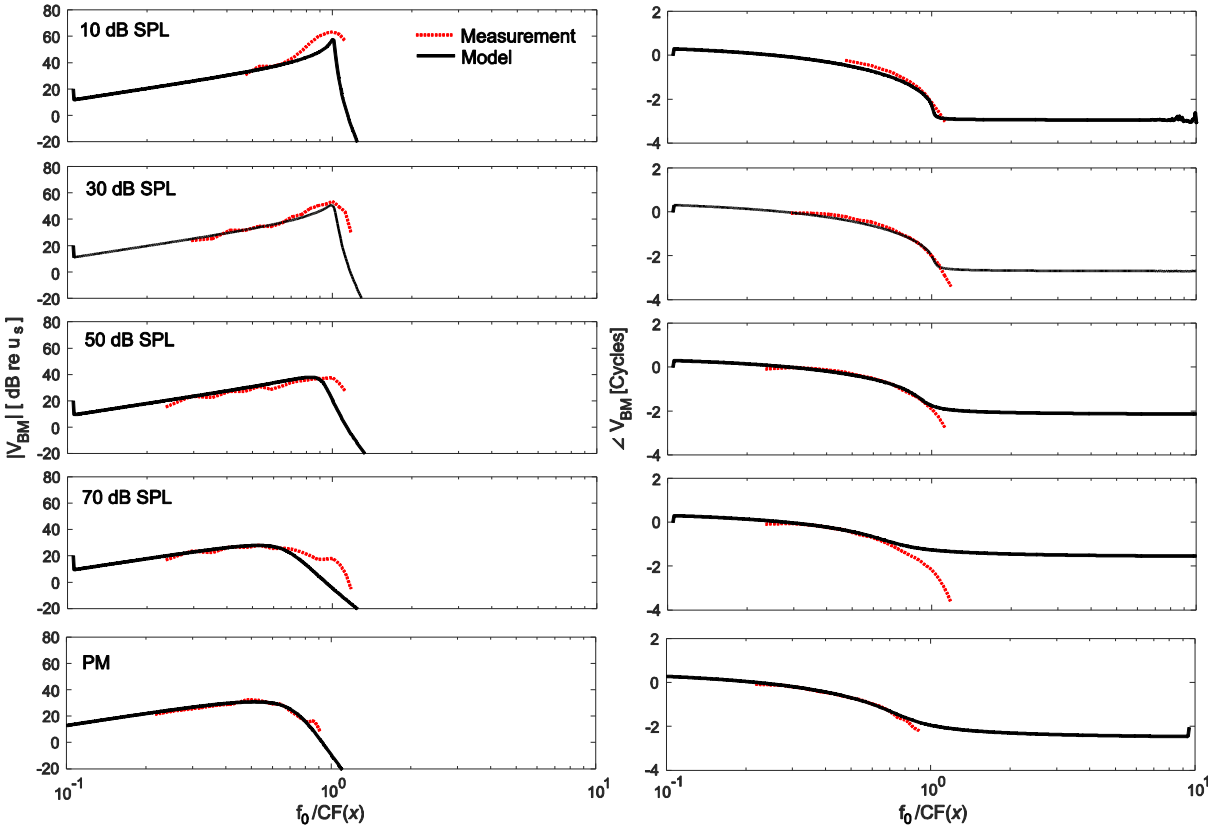

Figure 8 Comparison between the magnitudes and phases of the measured BM response is measured by Lee *et al*. (2015) for a CF of 9 kHz and SPLs of 10, 30, 50 and 70 dB, solid lines, and the response of a model with single degree-of-freedom micromechanics and 1D fluid coupling, obtained after optimisation to identify the micromechanical polls and zeros, dashed line.

V. POLES AND ZEROS OF THE FITTED MICROMECHANICAL MODEL WITH 3D FLUID COUPLING

The 1D model used for the coupling in the fluid chambers above only accounts for pressures that are uniform across the cross-section (de Boer, 1996). In reality the fluid pressure varies

over the cross-section of the duct, particularly near the characteristic place, where an additional near field pressure is produced close to the BM (de Boer, 1981; Elliott *et al.*, 2011). The effects of this near field pressure can be accounted for to some extent in the 1D model by increasing the apparent value of the BM mass to account for this fluid loading. It is interesting however to investigate whether a significantly better fit can be obtained to the measured BM response data if a 3D fluid coupling model is assumed. This can be readily incorporated into the elemental box model by adding exponentially varying near field components to the columns of the fluid coupling matrix, as shown in Figure 1 of Ni and Elliott (2015).

Figure 9 shows the results of fitting the measured data at a point along the cochlea with a CF of 9 kHz with a model that includes two degree-of-freedom micromechanics and 3D fluid coupling. The real and imaginary parts of the poles and zeros for similar models fitted to measured data at the four positions measured by Lee *et al*. (2015) are plotted as a function of excitation level in Figure 10. In this case the overall mass identified for the model, m_1 in equation (4), is only about 0.03 kg/m^2, since the additional mass due to fluid loading is accounted for in the 3D fluid coupling model. The values of the parameters in Figure 10 for the first pair of poles, and their variation with excitation level, are rather less consistent across the four sets of data than with the 1D fluid coupling, as shown in Figure 5, although now the position of the zero does seem to be more consistent.

The positions of the individual poles and zeros for the results measured at the position with a CF of about 9 kHz were again selected as being representative and are plotted in Figure 11. In this case there are two distinct pairs of poles evident at low SPLs, but they are no longer nearly coincident, with one pair of poles having an undamped natural frequency well above CF. At higher SPLs one pair of poles becomes almost coincident with the pair of zeros, so that the overall behaviour is close to that of a single degree-of-freedom system. Thus the poles no longer move at right angles to the frequency axis with increasing level, as they did in the case with 1D fluid coupling. Nevertheless, when the impulse responses are calculated from the fitted BM frequency responses in Figure 9, as shown by the dashed lines in Figure 7,they have a very similar form to those calculated from the BM frequency responses assuming 1D fluid coupling, with the positions of the first few peaks being nearly invariant of excitation level below 70 dB, since the fitted BM frequency responses in Figures 4 and 9 are so similar. The fact that the poles and zeros of the BM admittance are rather different when 1D and 3D fluid coupling is assumed clearly demonstrates that the modelled dynamic behaviour of the BM is different in these two cases.

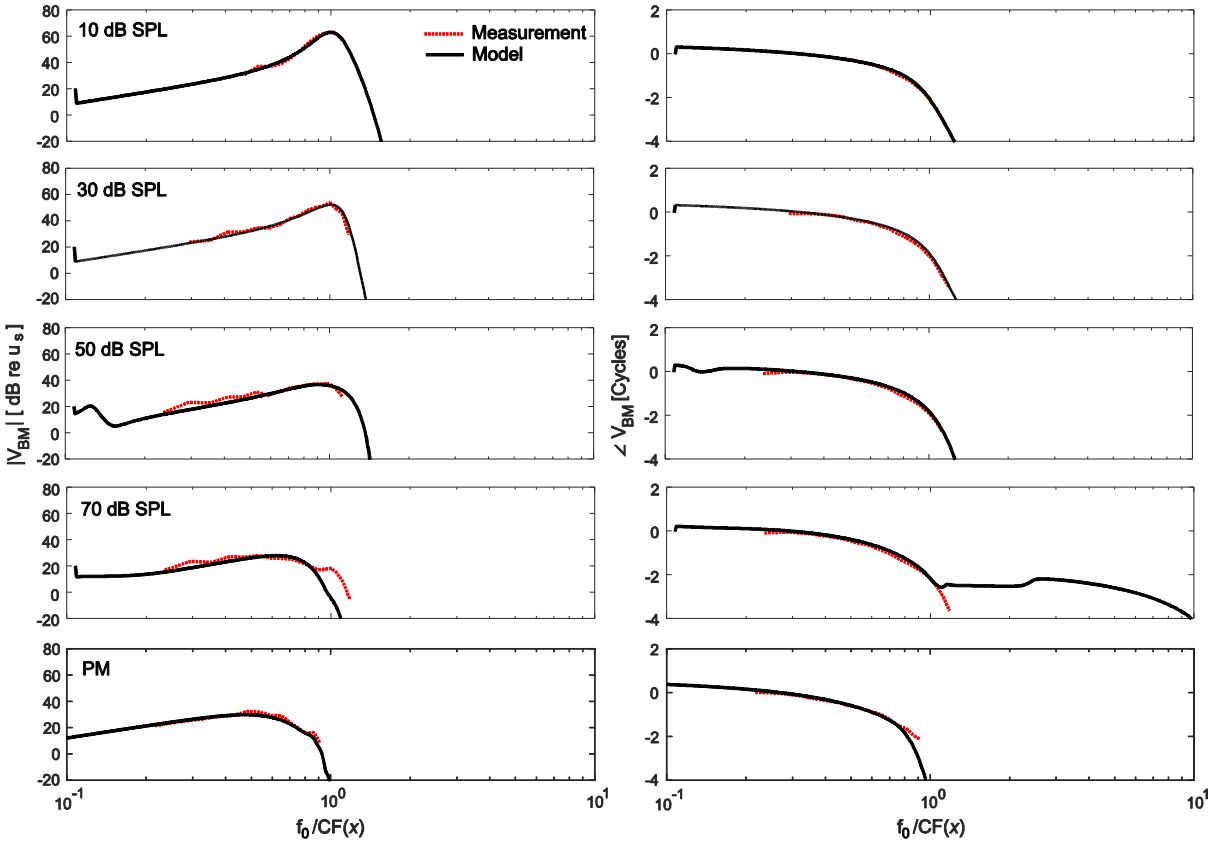

Figure 9 Comparison between the magnitudes and phases of the measured BM response is measured by Lee *et al*. (2015) for a CF of 9 kHz and SPLs of 10, 30, 50 and 70 dB, solid lines, and the response of a model with two degree-of-freedom micromechanics and 3D fluid coupling, obtained using multi-objective optimisation to identify the micromechanical polls and zeros, dashed line.

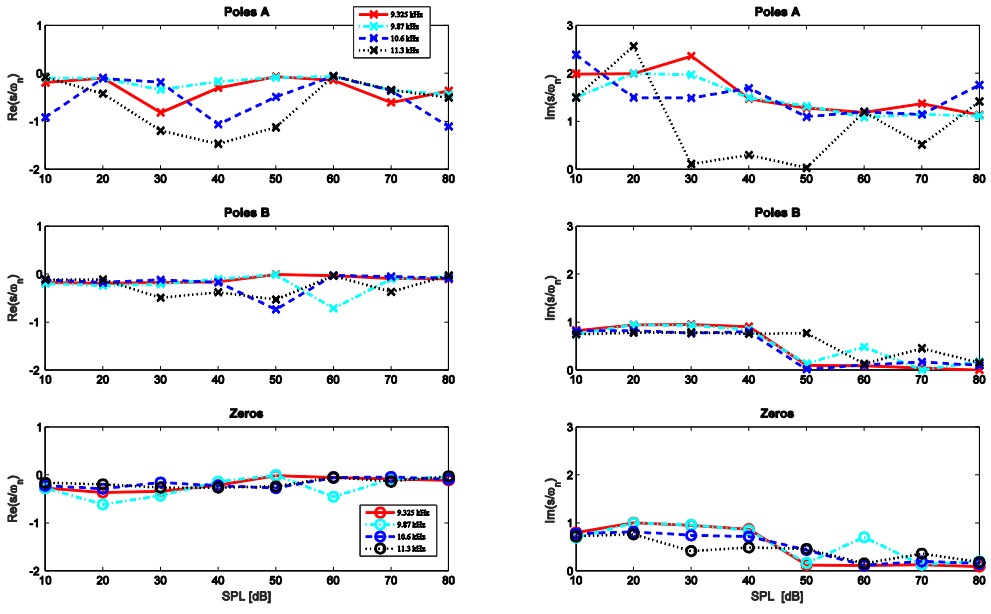

Figure 10 (colour online) The real and imaginary parts of the poles and zeros calculated using a fitted model, based on measurement data by Lee *et al*. (2015), with two degree-of-freedom micromechanics and 3D fluid coupling, as a function of excitation level.

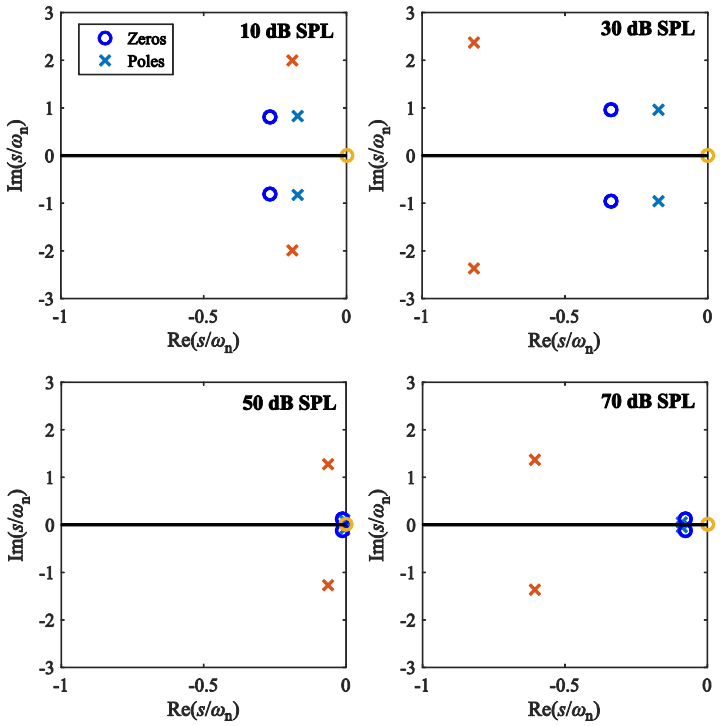

Figure 11 (colour online) Real and imaginary parts of the poles, ×, and zeros, o, calculated from the two degree-of-freedom model with 3D fluid coupling based on measurement data from Lee *et al*. (2015) for a CF of 9 kHz and SPLs of 10, 30, 50 and 70 dB.

VI. Modelling Error

The value of the normalised mean square error defined by equation (14), averaged across the fits for the four measurement points for the various different cases of micromechanical model and fluid coupling, are plotted as a function of excitation level in Figure 12. It can be seen that the mean square error when the cochlear model includes 3D fluid coupling is generally lower than when the model assumes 1D fluid coupling. Most striking, however, is the difference between the errors with the single and two degree-of-freedom micromechanics. This is particularly true at low levels, as expected, since the active cochlea cannot be accurately represented using single degree-of-freedom micromechanics. The mean square error with two degree-of-freedom micromechanics is also about one third of that found using single degree-of-freedom micromechanics at higher excitation levels, however, suggesting that the largest SPL used in these experiments was not sufficiently high to prevent some residual feedback behaviour. This residual feedback behaviour can be interpreted as being due to the feedback gain, γ, not being entirely zero, and thus having an effect on the parameters of equation (10), even though the real part of the admittance in this equation may be entirely positive, so that the system is passive. This is confirmed by the results from the post-mortem measurements of Lee *et al*. (2015) that are also shown in Figure 12. In this case the error is almost as small for the

one degree-of-freedom model as it is for the two degree-of-freedom model, so that only one degree-of-freedom is required for this passive case.

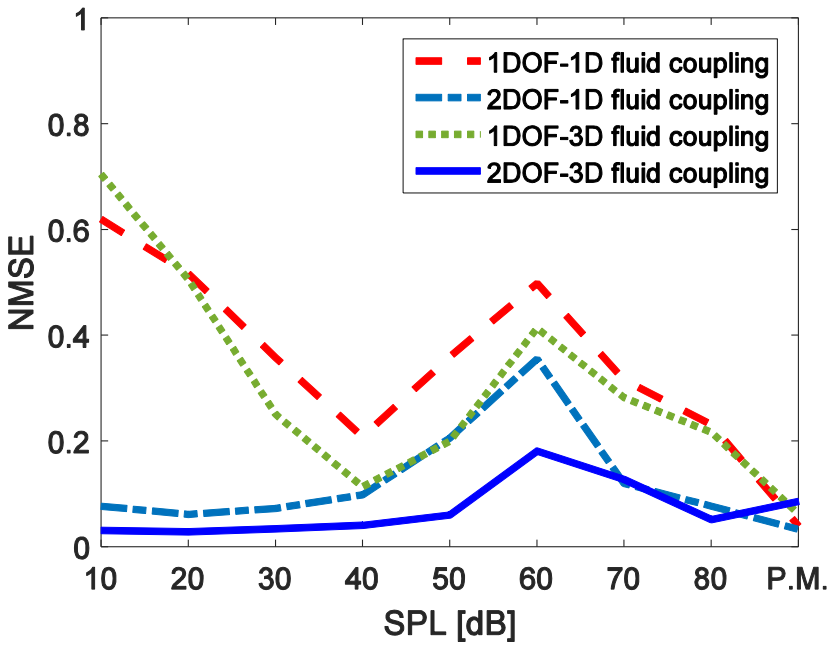

Figure 12 (colour online) The averaged distribution of the normalised mean square error, NMSE, as a function of excitation level, SPL, of different types of model when optimised to fit the measured BM response measured by Lee *et al*. (2015), averaged over four closely spaced locations along the cochlea.

VII. DISCUSSION AND CONCLUSIONS

The mechanical response of the cochlea depends on the micromechanical response of the basilar membrane and organ of Corti, coupled by the fluid in the scalae. A number of lumped parameter mechanical models of the micromechanics have been proposed, typically with a single degree-of-freedom for the passive case and two degree-of-freedom for the active case. A general form of the active two degree-of-freedom micromechanical model is shown to require 10 parameters to specify its quasi-linear response, whereas, if its admittance is expressed in terms of its poles and zeros, it can be specified by only 7 parameters. This is the smallest possible number of parameters required to specify the response and thus allow such a pole-zero model to be uniquely fitted to measured data.

The fitting procedure is complicated by the need to make assumptions about how the micromechanical admittance varies along the cochlea and the need to combine the micromechanical response with a model of the fluid coupling to give the overall mechanical response of the cochlea. Scaling symmetry is invoked to calculate the variation of micromechanical admittance along the cochlea and either 1D or 3D fluid coupling is assumed

in an elemental box model of the cochlea to calculate the coupled response. A numerical optimisation approach is then used to adjust the pole and zero positions in the model so that it best fits the responses measured in the intact mouse cochlea by Lee *et al*. (2015), using a least mean square error criterion. The measured cochlea response changes with excitation level, and so separate pole-zero models of the micromechanics are used for the eight values of SPL at which the measurements were made.

Initially, using a two degree-of-freedom micromechanical model with 1D fluid coupling, it is shown that a reasonable fit to both the magnitude and phase of the measured BM responses can be obtained for all excitation levels, although the fit at low SPLs is slightly better than it is at high SPLs. This is in contrast to the case in which a single degree-of-freedom micromechanical model is assumed, in which case the fit is significantly better at high SPLs than it is at low SPLs, since in this case the model can only approximate the passive micromechanical behaviour. Lee *et al*. (2015) provide data for the responses measured at four closely spaced positions along the cochlea, each at eight values of SPL. Using scaling symmetry again, it is found that the variation of the pole and zero positions with SPL are similar for the models fitted at each of these positions, which gives some confidence in the repeatability of the model and the fitting procedure. It is found that for post-mortem results the fit is similar with one and two degree-of-freedom micromechanical models, indicates that the addition degree-of-freedom is unnecessary in this case and, as expected, a single degree-of-freedom model is sufficient.

Single and two degree-of-freedom models are also fitted to the measured data using 3D fluid coupling in the cochlea model. The fit between the model response and the measured data is quantified in terms of the normalised mean square error, NMSE, averaged over all four measurement positions. This is generally lower if 3D fluid coupling, rather than 1D fluid coupling, is assumed, but the two degree-of-freedom micromechanical model still gives a significantly lower NMSE than the single degree-of-freedom model.

All models have a somewhat larger NMSE for excitation levels corresponding to an SPL of around 60 dB than at higher or lower SPLs. It is not clear whether this is a limitation of the model, or some aspect of the measured responses in this case. It is interesting, however, to note that the nonlinear input-output level curves for the BM response measured close to CF, as reviewed by Robles and Ruggero (2001) for example, have the smallest slope, corresponding to the greatest degree of compression, at about 60 dB SPL. A similar effect was also observed in DPOAE input-output curves and in the loudness function by Neely *et al*. (2003), indicating

that the cochlear response is at its most nonlinear at about 60 dB SPL. This is consistent with the finding that the feedback gain in previous quasi-linear models changes most rapidly with level for excitations of around 60 dB SPL (Kanis and de Boer, 1993; Liu and Liu, 2016). NMSEs at the highest excitation levels used in the measurements of Lee *et al*. (2015), at 80 dB SPL, are similar with either 1D or 3D fluid coupling, for both single degree-of-freedom and two degree-of-freedom micromechanical models. The overall level of the NMSE for the two degree-of-freedom model is still significantly lower at 80 dB SPL than that of the single degree-of-freedom model, however, suggesting that the cochlea is not behaving entirely passively at this excitation level.

While a given mechanical system can always be uniquely represented in terms of its poles and zeros, a pole-zero model generally cannot be said to correspond to a unique mechanical system, particularly if there is feedback involved. The pole-zero results obtained by fitting to measured data at a single point thus cannot be used to derive a unique lumped parameter model for the micromechanics. They do, however, give an indication of the type of behaviour required of such a lumped parameter model, both in terms of the order of this model and in terms of the way in which its pole and zero positions should vary with excitation level.

ACKNOWLEDGMENT

The authors declare no existing or potential conflict of interest. Guangjian Ni was supported by grants from EPSRC (Engineering nonlinearity, Grant No. EP/K003836/1) and MRC (Interaction between sensory and supporting cells in the organ of Corti: basis for sensitivity and frequency selectivity of mammalian cochlea, Grant No. MR/N004299/1).

REFERENCES

Baumgart, J., Chiaradia, C., Fleischer, M., Yarin, Y., Grundmann, R., and Gummer, A. W. (**2008**). "Fluid mechanics in the subtectorial space," in Concepts and Challenges in the Biophysics of Hearing, Proceedings of the 10th International Workshop on the Mechanics of Hearing, edited by N. P. Cooper, and D. T. Kemp (World Scientific, Keele University, Staffordshire, UK), pp. 288-293.

Böhnke, F., and Arnold, W. (**1999**). "3D-Finite Element Model of the Human Cochlea Including Fluid-Structure Couplings," ORL-J. Oto-Rhino-Laryngol. Head Neck Surg. **61**, 305-310.

Cai, H., and Chadwick, R. (**2003**). "Radial structure of traveling waves in the inner ear," SIAM J. Appl. Math. **63**, 1105-1120.

Cai, H., Shoelson, B., and Chadwick, R. S. (**2004**). "Evidence of tectorial membrane radial motion in a propagating mode of a complex cochlear model," Proc. Natl. Acad. Sci. U. S. A. **101**, 6243-6248.

Choudhury, N., Song, G., Chen, F., Matthews, S., Tschinkel, T., Zheng, J., Jacques, S. L., and Nuttall, A. L. (**2006**). "Low coherence interferometry of the cochlear partition," Hear. Res. **220**, 1-9.

de Boer, E. (**1980**). "Auditory physics. Physical principles in hearing theory. I," Phys. Rep.-Rev. Sec. Phys. Lett. **62**, 87-174.

de Boer, E. (**1981**). "Short waves in three-dimensional cochlea models: Solution for a 'block' model," Hear. Res. **4**, 53-77.

de Boer, E. (**1995**). "The "inverse problem" solved for a three-dimensional model of the cochlea. II. Application to experimental data sets," J. Acoust. Soc. Am. **98**, 904-910.

de Boer, E. (**1996**). "Mechanics of the cochlea: Modelling efforts," in The cochlea, edited by P. Dallos, A. N. Popper, and R. R. Fay (Springer, New York), pp. 258-317.

de Boer, E. (**1997**). "Connecting frequency selectivity and nonlinearity for models of the cochlea," Aud. Neurosci. **3**, 377-388.

Diependaal, R. J., Viergever, M. A., and de Boer, E. (**1986**). "Are active elements necessary in the basilar membrane impedance?" J. Acoust. Soc. Am. **80**, 124-132.

Elliott, S. J., Ku, E. M., and Lineton, B. (**2007**). "A state space model for cochlear mechanics," J. Acoust. Soc. Am. **122**, 2759-2771.

Elliott, S. J., Lineton, B., and Ni, G. (**2011**). "Fluid coupling in a discrete model of cochlear mechanics," J. Acoust. Soc. Am. **130**, 1441-1451.

Elliott, S. J., and Ni, G. (**2014**). "Near Field Fluid Coupling between Internal Motion of the Organ of Corti and the Basilar Membrane," in Proceedings of the 12th International Workshop on the Mechanics of Hearing, edited by Karavitaki, K. D. and Corey, D. P.

Elliott, S. J., Tehrani, M. G., and Langley, R. S. (**2015**). "Nonlinear damping and quasi-linear modelling," Proc. R. Soc. A-Math. Phys. Eng. Sci. **373**.

Elliott, S. J., Ni, G., and Sun, L. (**2017**). "Fitting Pole-zero Micromechanical Models to Cochlear Response Measurements," in Mechanics of Hearing 2017 workshop, 19–24 June 2017, Ontario, Canada.

Gao, S. S., Raphael, P. D., Wang, R., Park, J., Xia, A., Applegate, B. E., and Oghalai, J. S. (**2013**). "In vivo vibrometry inside the apex of the mouse cochlea using spectral domain optical coherence tomography," Biomed. Opt. Express **4**, 230-240.

Geisler, C. D. (**1993**). "A realizable cochlear model using feedback from motile outer hair cells," Hear. Res. **68**, 253-262.

Greenwood, D. D. (**1990**). "A cochlear position-frequency function for several species – 29 years later," J. Acoust. Soc. Am. **87**, 2592-2605.

Hubbard, A. E., and Mountain, D. C. (**1996**). "Models of the Cochlea," in Auditory Computation, edited by H. L. Hawkins, T. A. McMullen, A. N. Popper, and R. R. Fay (Springer-Verlag, New York), pp. 62-120.

Kanis, L. J., and de Boer, E. (**1993**). "Self-suppression in a locally active nonlinear model of the cochlea: A quasilinear approach," J. Acoust. Soc. Am. **94**, 3199-3206.

Keiler, S., and Richter, C. P. (**2001**). "Cochlear dimensions obtained in hemicochleae of four different strains of mice: CBA/CaJ, 129/CD1, 129/SvEv and C57BL/6J," Hear. Res. **162**, 91-104.

Kolston, P. J., and Ashmore, J. F. (**1996**). "Finite element micromechanical modeling of the cochlea in three dimensions," J. Acoust. Soc. Am. **99**, 455-467.

Kozlov, A. S., Baumgart, J., Risler, T., Versteegh, C. P. C., and Hudspeth, A. J. (**2011**). "Forces between clustered stereocilia minimize friction in the ear on a subnanometre scale," Nature **474**, 376-379.

Kuo, F. F. (**1966**). Network Analysis and Synthesis (John Wiley and Sons, New York).

Lee, H. Y., Raphael, P. D., Park, J., Ellerbee, A. K., Applegate, B. E., and Oghalai, J. S. (**2015**). "Noninvasive in vivo imaging reveals differences between tectorial membrane and basilar membrane traveling waves in the mouse cochlea," Proc. Natl. Acad. Sci. U. S. A. **112**, 3128-3133.

Lee, H. Y., Raphael, P. D., Xia, A., Kim, J., Grillet, N., Applegate, B. E., Ellerbee Bowden, A. K., and Oghalai, J. S. (**2016**). "Two-Dimensional Cochlear Micromechanics Measured In Vivo Demonstrate Radial Tuning within the Mouse Organ of Corti," J. Neurosci. **36**, 8160-8173.

Liu, Y. W. (**2014**). "Stationary noise responses in a nonlinear model of cochlear mechanics: iterative solutions in the frequency domain," J. Acoust. Soc. Am. **136**, 1788-1796.

Liu, Y. W., and Neely, S. T. (**2009**). "Outer hair cell electromechanical properties in a nonlinear piezoelectric model," J. Acoust. Soc. Am. **126**, 751-761.

Liu, Y. W., and Liu, T. C. (**2016**). " Quasilinear reflection as a possible mechanism for suppressor-induced otoacoustic emission," J. Acoust. Soc. Am. **140**, 4193-4203.

Mammano, F., and Ashmore, J. F. (**1993**). "Reverse transduction measured in the isolated cochlea by laser Michelson interferometry," Nature **365**, 838-841.

Mandal, S., Zhak, S. M., and Sarpeshkar, R. (**2009**). "A Bio-Inspired Active Radio-Frequency Silicon Cochlea," IEEE J. Solid-State Circuit **44**, 1814-1828.

Neely, S. T. (**1981**). "Finite difference solution of a two-dimensional mathematical model of the cochlea," J. Acoust. Soc. Am. **69**, 1386-1393.

Neely, S. T. (**1985**). "Mathematical modelling of cochlear mechanics," J. Acoust. Soc. Am. **78**, 345-352.

Neely, S. T., and Kim, D. O. (**1986**). "A model for active elements in cochlear biomechanics," J. Acoust. Soc. Am. **79**, 1472-1480.

Neely, S. T., Gorga, M. P. and Dorn, P. A. (**2003**). " Cochlear compression estimates from measurements of distortion-product otoacoustic emissions," J. Acoust. Soc. Am. **114**, 1499-1507.

Ni, G., and Elliott, S. J. (**2015**). "Comparing methods of modeling near field fluid coupling in the cochlea," J. Acoust. Soc. Am. **137**, 1309-1317.

Ni, G., Elliott, S. J., and Baumgart, J. (**2016**). "Finite-element model of the active organ of Corti," J. R. Soc. Interface **13**.

Nilsen, K. E., and Russell, I. J. (**2000**). "The spatial and temporal representation of a tone on the guinea pig basilar membrane," Proc. Natl. Acad. Sci. U. S. A. **97**, 11751-11758.

Nuttall, A. L., Dolan, D. F., and Avinash, G. (**1991**). "Laser Doppler velocimetry of basilar membrane vibration," Hear. Res. **51**, 203-213.

Ren, T. (**2002**). "Longitudinal pattern of basilar membrane vibration in the sensitive cochlea," Proc. Natl. Acad. Sci. U. S. A. **99**, 17101-17106.

Ren, T., and Nuttall, A. L. (**2001**). "Basilar membrane vibration in the basal turn of the sensitive gerbil cochlea," Hear. Res. **151**, 48-60.

Rhode, W. S. (**1971**). "Observations of the vibration of the basilar membrane in squirrel monkeys using the Mossbauer technique," J. Acoust. Soc. Am. **49**, 1218-1231.

Robles, L., and Ruggero, M. A. (**2001**). "Mechanics of the Mammalian Cochlea," Physiol. Rev. **81**, 1305-1352.

Sellick, P. M., Patuzzi, R., and Johnstone, B. M. (**1982**). "Measurement of basilar membrane motion in the guinea pig using the Mössbauer technique," J. Acoust. Soc. Am. **72**, 131-141.

Shera, C. A. (**2001**). "Intensity-invariance of fine time structure in basilar-membrane click responses: Implications for cochlear mechanics," J. Acoust. Soc. Am. **110**, 332-348.

Shera, C. A. (**2007**). "Laser amplification with a twist: Traveling-wave propagation and gain functions from throughout the cochlea," J. Acoust. Soc. Am. **122**, 2738-2758.

Steele, C. R., and Taber, L. A. (**1979**). "Comparison of WKB calculations and experimental results for three-dimensional cochlear models," J. Acoust. Soc. Am. **65**, 1007-1018.

Sun, L., Elliott, S. J., and Ni, G. (**2015**). "Fitting Pole-zero Micromechanical Models to Coupled Cochlear Responses by Direct Optimization," in Proceedings of the 22th International Congress on Sound and Vibration, edited by M. J. Crocker, M. Pawelczyk, F. Pedrielli, E. Carletti, and S. Luzzi, p. 8.

Thorne, M., Salt, A. N., DeMott, J. E., Henson, M. M., Henson, O. W., Jr., and Gewalt, S. L. (**1999**). "Cochlear fluid space dimensions for six species derived from reconstructions of three-dimensional magnetic resonance images," Laryngoscope **109**, 1661-1668.

Wang, R. K., and Nuttall, A. L. (**2010**). "Phase-sensitive optical coherence tomography imaging of the tissue motion within the organ of Corti at a subnanometer scale: a preliminary study," J. Biomed. Opt. **15**, 056005.

Wang, Y., Steele, C. R., and Puria, S. (**2016**). "Cochlear Outer-Hair-Cell Power Generation and Viscous Fluid Loss," Sci. Rep. **6**, 19475.

Watts, L. (**2000**). "The mode-coupling Liouville-Green approximation for a two-dimensional cochlear model," J. Acoust. Soc. Am. **108**, 2266-2271.

Warburton, G. B. (**1976**). The dynamic behaviour of structures, 2nd, (Pergamon Press, Oxford).

Zweig, G. (**1991**). "Finding the impedance of the organ of Corti," J. Acoust. Soc. Am. **89**, 1229-1254.

Zweig, G. (**2015**). "Linear cochlear mechanics," J. Acoust. Soc. Am. **138**, 1102-1121.